

# Automatic Generation of Dynamic 3D Models for Medical Segmentation Tasks

Lars Dornheim<sup>1</sup>, Jana Dornheim<sup>1</sup>, Klaus D. Tönnies<sup>1</sup>

<sup>1</sup>Department of Simulation and Graphics, Faculty of Computer Science, Otto-von-Guericke University Magdeburg, Germany

## ABSTRACT

Models of geometry or appearance of three-dimensional objects may be used for locating and specifying object instances in 3D image data. Such models are necessary for segmentation if the object to be segmented is not separable based on image information only. They provide a-priori knowledge about the expected shape of the target structure. The success of such a segmentation task depends on the incorporated model knowledge.

We present an automatic method to generate such a model for a given target structure. This knowledge is created in the form of a 3D Stable Mass-Spring Model (SMSM) and can be computed from a single sample segmentation. The model is built from different image features using a bottom-up strategy, which allows for different levels of model abstraction.

We show the adequacy of the generated models in two practical medical applications: the anatomical segmentation of the left ventricle in myocardial perfusion SPECT, and the segmentation of the thyroid cartilage of the larynx in CT datasets. In both cases, the model generation was performed in a few seconds.

**Keywords:** Stable Mass Spring Models, model generation, model-based segmentation, segmentation, shape

## 1. INTRODUCTION

In many medical segmentation tasks, especially in 3D, complex shapes have to be handled. Shape knowledge about the segmentation target structures is necessary, when image information is incomplete or inhomogeneous.

Shape knowledge can be incorporated into the segmentation process by means of model-based segmentation techniques. In the last years, two major classes of model shape-based segmentation techniques have evolved. On the one hand, there are *stochastic models* like Active Shape Models,<sup>1</sup> on the other hand there are *dynamic models* like e.g. Active Contours.<sup>2</sup>

In this paper, we focus on dynamic models, especially on *Stable Mass Spring Models* (SMSMs).<sup>3</sup> These models are able to model complex shape knowledge explicitly and are parameterized locally. This allows for a detailed adaptation to local image features, as well as for local corrections and intervention by the user. It should be kept in mind, that applying SMSMs to segmentation is different from simulation applications such as those reported in.<sup>4</sup> The SMSM approach has not the intention to simulate a real-world scenario, but to find the structures in the given image data.

In contrast to stochastic models deducing their model knowledge from a large sample database, dynamic models use a single reference model that adapts to the data iteratively by a local optimization process. The model must be designed such that virtual image forces attract it to its segmentation target structure.

Up to now, such reference models had to be provided manually for every application,<sup>5</sup> which is a tedious and error-prone task. It often has the consequence, that only very simple models are used, which are insufficient for modelling complex shapes. As the segmentation quality depends directly on the adequacy and exactness of the employed model, an automatic model generation is desirable.

## 2. RELATED WORK

For most applications, dynamic segmentation models are created manually.<sup>5</sup> An automatic generation of 3D models is limited to an initial adaption of a general surface mesh to an object for segmentation or reconstruction.<sup>6</sup> So, no model knowledge is incorporated permanently into the model, which could be used for the segmentation of similar structures later on.

A recent approach utilizes growing cell neural networks for the creation of 3D surface point distribution models.<sup>7</sup> It is a heuristic technique that uses a self-organizing network to determine landmark counts and positions during an unsupervised learning process. This approach has some similarities to the one in,<sup>8</sup> where also landmarks for a statistical segmentation approach were tried to be constructed automatically, but here 3D deformable surface meshes are used instead of growing cell neural networks. In both cases, a model containing landmarks is created on a chosen segmentation and then adapted to the other training segmentations. Finally, this set of landmarks is adapted automatically to all training samples. The two approaches create surface models for intermediate use, which are intended to work on binary segmentation masks and not on real data. The emphasis in these two approaches lies on statistical segmentation methods.

To our knowledge, no method is reported that focuses on the construction of explicit deformable models (active contours, mass-spring models, etc.).

## 3. STABLE MASS SPRING MODELS

Our model, the SMSM (Stable Mass-Spring Model<sup>3</sup>), is a three-dimensional mass-spring model, which is a dynamic system consisting of masses connected by elastic springs. The masses are associated with sensors converting image features to forces that act on the masses and drive the model adaptation.

As opposed to other mass-spring models, SMSMs have an additional constraint ensuring the model's shape stability: besides the well-known spring forces controlling the model's size, so-called *torsion forces* are introduced, controlling the 3D shape by adjusting the *spring directions* according to a reference system (mass, model or world). The introduction of torsion forces allows for stable models with weak cross-linking, because deformation is represented explicitly, instead of controlling it indirectly by introducing extra springs. The condition of weak cross-linking is also necessary, if size and shape flexibility of an SMSM shall be controlled independently, which is generally desirable.

## 4. REQUIREMENTS FOR MODEL GENERATION

We found that the following requirements need to be fulfilled by the described SMSMs for a robust, straight and correct segmentation:

- (a) The sensors (and therefore the masses) should be distributed well across the 3D shape, preserving significant features (e.g. thin, long model parts).
- (b) The cross-linking of the sensors should be stable, local and well-balanced.
- (c) At the boundaries of the modelled structure, faces should be placed in the model, representing its outline.

Point (a) is important for quality and efficiency of the resulting segmentation, because the sensor positions are the only points at which the model can directly access the data. Therefore a minimal set of masses is needed, describing every necessary feature for a given abstraction level.

Point (b) strives for shape stability, which is nearly always given for SMSMs, as well as for well-balanced cross-linking, making the different forces act evenly in all model parts. Furthermore, local connectivity is required to ensure a true local behavior of this model approach.

Since SMSMs are not necessarily surface models, a surface mesh has to be explicitly defined for them (by faces, see point (c)). So, the latter segmentation boundary can be determined after segmentation.

We identified the following requirements for the model generation process:

- (I) The model should be generated based on a single dataset with a verified segmentation.
- (II) The abstraction level of the model should be configurable.
- (III) The model generation should run automatically and efficiently.

## 5. MODEL GENERATION

We developed a heuristic method to automatically generate SMSMs with the properties (a) - (c) mentioned in section 4. Input to this process is primarily one sample segmentation given as a binary voxel dataset. Its regions and region boundaries are features that will automatically be coded in the model.

The generated model is composed of different submodels, (also called sensor groups, because of the same type of sensor throughout each group). We differentiate two kinds of submodels:

1. *Volumetric submodels* represent nearly homogeneous regions. Here, the masses are arranged in a 3D volume. Their sensors are attracted by special intensity values in the dataset.
2. *Surface submodels* represent borders of regions. Here, the masses form a surface in 3D, while their sensors search for contour information in the image dataset.

The model generation method consists of the following four steps: Region marking, volumetric and surface submodel creation and model assembly. We will demonstrate these steps based on a task of registering an anatomical model of the left ventricle to 3D myocardial perfusion SPECT data of the heart, which can be considered as a model-based segmentation of the ventricle perfusion using a model of a healthy heart, where perfusion corresponds to ventricle anatomy.

### 5.1. Region marking

Regions that are supposed to be represented in the model are marked. A model may consist of several different regions, which are represented by different (volumetric) submodels. In the case of the left ventricle, two regions were used (ventricle wall and blood pool) (figure 1c). In the case of the thyroid cartilage, only one region (the cartilage itself) was used.

Marking of regions, that are not the object itself, can be achieved by filling algorithms or by means of Boolean operations with the convex hull. In case of convex hull algorithms, often small artifact groups evolve, due to not completely convex object boundaries. These artifacts can be removed efficiently by defining the voxel set as a node set of a graph with edges connecting neighboring voxels of the same color and then deleting connected components with a node count smaller than a certain threshold (see figure 1 for an illustration of the whole process).

### 5.2. Volumetric submodel creation

For each region, a volumetric submodel is created. Its masses are supposed to cover the whole region, representing the expected intensities at the individual sensor positions. The sensor density should be adjustable by the user, depending on the desired abstraction level of the model. Thereto, the sensors need to be placed evenly all over the given region, while preserving specific features of the modelled shape (like e.g. the thin and long cornu superii and inferii of the thyroid cartilage).

For this purpose, all masses are first placed on an equidistant grid across the region with a high density (figure 2a). Then, the number of sensors is reduced iteratively. This is achieved by repeatedly moving each sensor to the centroid of all sensors in a fix-sized neighborhood around it. Sensors occupying the same place are merged. This process will apparently converge on every bounded set with a finite step count to a well-distributed group of sensors (figure 2b), whose density depends only on the size of the centroid neighborhood. After convergence, the final set of sensors for this region is reached.

Every sensor is now provided with an intensity to search for, which is taken directly from its position in the dataset corresponding to the input segmentation. These sensors are not only sensing one special target intensity,

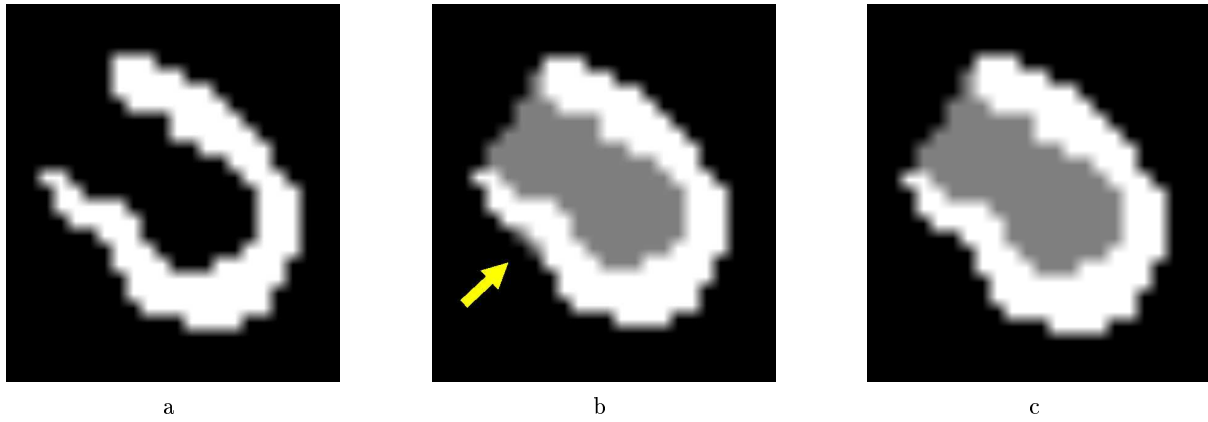


**Figure 1.** (a) shows the slice of a binary segmentation of a left ventricle. White region represents object shape. (b) shows an artefact (gray, arrow) created during inner region marking (gray). (c) shows the inner region marked (gray) with artefacts removed.

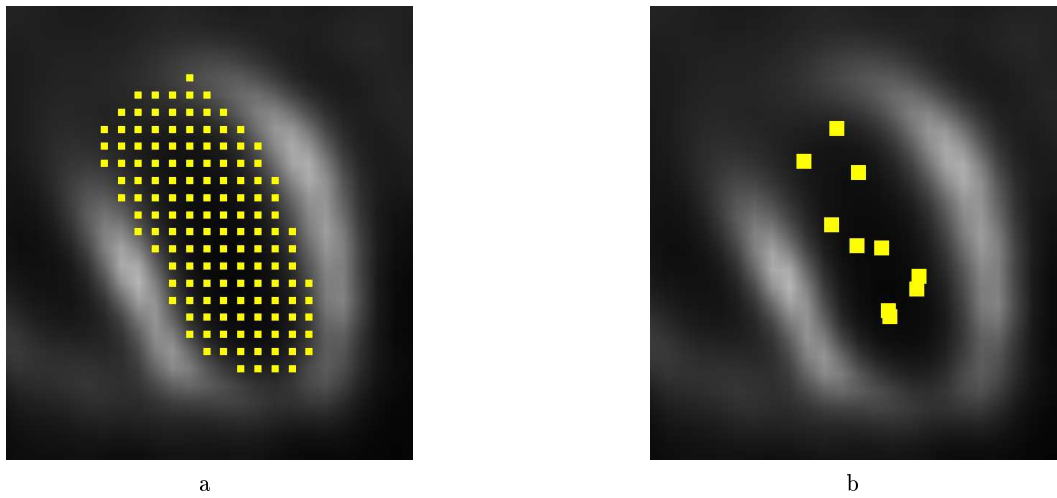


**Figure 2.** (a) shows the starting grid of the intensity sensors in the LV inner region and (b) shows the final alignment. Both images show projections of a certain depth range.

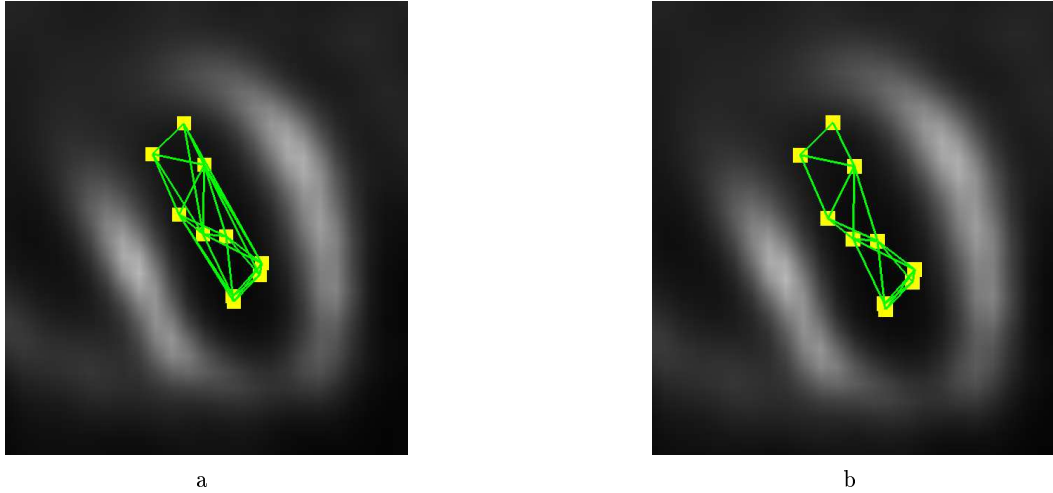


**Figure 3.** (a) shows the delaunay triangulation of the intensity sensor group in the LV inner region and (b) shows the pruned interconnection. Both images show projections of a certain depth range.

but have a force peak on it. The more an intensity of a voxel is different from this target intensity, the weaker is the force acting on that sensor in direction of this voxel.

Alternatively, these target intensities can be given directly, making the model more abstract. We did the latter for our experiments, as we knew what the model parts should be searching for (e.g. white LV wall and black LV interior) and the single datasets did not contain these intensities so well at all positions.

Finally, cross-linking of the volumetric sensor group is achieved by means of a three-dimensional Delaunay triangulation (figure 3a) to make a complete and stable interconnection that partitions the volume efficiently and completely into simplices. This way, every connection is an edge of a simplex and therefore prevented from going through the interior of other simplices. This makes most of the resulting spring connections relatively short. But some of these connections are sometimes still long, so that they have to be pruned such that only local connections remain in the model (figure 3b), ensuring only local force chains, which are motivated in point (b) of section 4.

### 5.3. Surface submodel creation

The surface submodel represents the boundary of a region by a mesh of contour sensors. These sensors have to be placed denser in regions rich of contour features.

First, a dense surface mesh of a region’s boundary is created via Marching Cubes (figure 4a). A sparser mesh is generated from this initial mesh by using a polygon mesh simplification method. We used Quadric Error Metrics simplification,<sup>9</sup> because it is efficient, easy to parametrize (mesh triangle reduction level = abstraction level) and leads to good results, i.e. the sensors were distributed well according to the mesh features to model (figure 4b).

After polygon reduction, large planar areas of the boundary may end up as large triangles without any inner nodes. In order to access image data at evenly-spaced sampling positions, additional sensor positions in planar surface areas could be needed. These large polygons are therefore split up repeatedly, until a given minimum density is reached.

Now, the final sensor mesh is created. All nodes in the mesh become masses with contour sensors. We use Active Sensors,<sup>10</sup> heading only for contours of the same normal directions as the local surface at each sensor position.

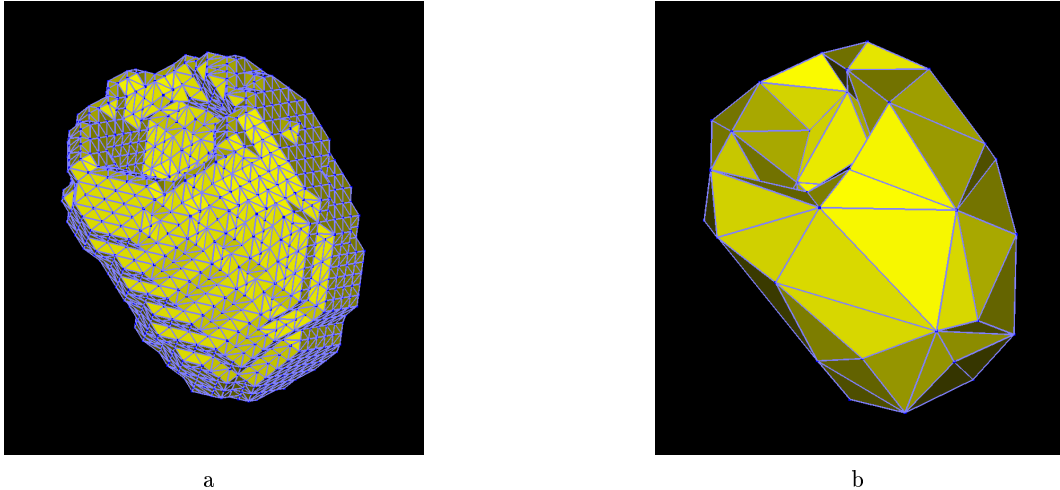


**Figure 4.** (a) shows the iso surface mesh of the wall region of the LV. (b) shows the reduced iso surface mesh via Quadric Error Metrics simplification.

#### 5.4. Model assembly

The last step is to assemble the complete model by connecting all volumetric and surface submodels, while maintaining the model’s local connectedness.

At first, adjacent volumetric submodels need to be interconnected locally. This is achieved by connecting only the *border sensors* of the two submodels, lying on the directly facing outer parts of both submodels. A border sensor is a sensor from one of the two submodels, which is the closest sensor in its submodel to at least one sensor in the other submodel. To connect two volumetric submodels, each border sensor is connected to its closest sensor of the other volumetric submodel (figure 5b).

Finally, all surface submodels are connected to their corresponding volumetric submodel by connecting every surface sensor to the closest sensor in the volumetric submodel (figure 5a). Because a surface submodel consists mainly of border sensors w.r.t. its associated volumetric submodel, this strategy results in a well-balanced, local interconnection between such sensor groups.

By these procedures, a complete and locally connected volumetric model of the segmentation target structure is created.

At last, the exact constructed model shape is anchored in the model for the segmentation process, which means making the current spring lengths and directions the rest lengths and rest directions of the corresponding springs.

## 6. RESULTS

We automatically generated models for two different applications. Both represent three-dimensional medical structures that usually have gaps in comparison with the ideal expected structure due to medical or imaging issues. These gaps have to be bridged by model knowledge.

### 6.1. Anatomical segmentation of the left ventricle in 3D-SPECT

In the first case, the left ventricle (LV) in myocardial perfusion SPECT images was to be segmented anatomically. The LV is not always completely depicted in SPECT data, because myocardial infarctions can cause whole parts of the left ventricle wall to be invisible. Thereto, we registered an anatomical model of the LV to the data, which leads to an anatomical segmentation of the LV, where functional LV wall gaps in the image data are bridged by model knowledge (figure 6a shows this in principle).

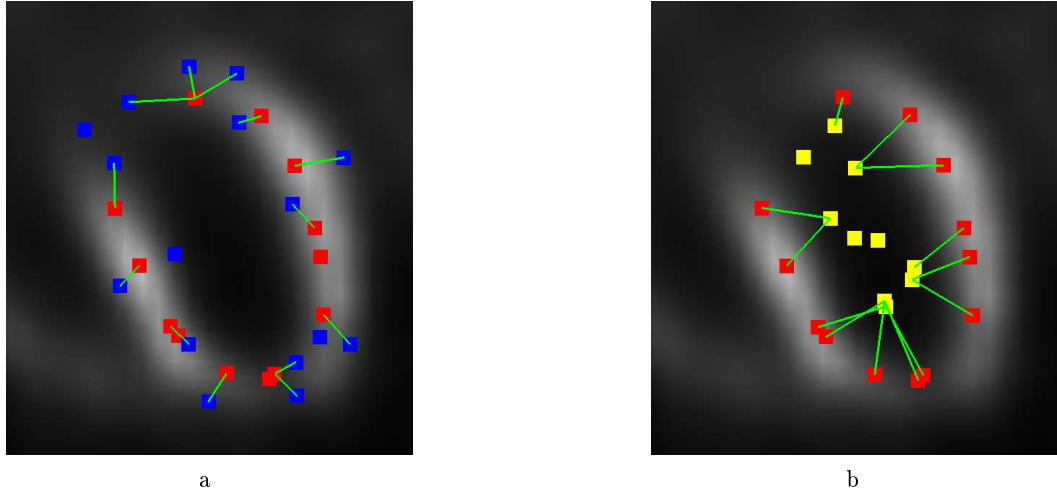


**Figure 5.** 2D projection view, only masses and springs lying fully within the projected depth range are displayed. **(a)**: connections of a surface sensor group (blue) to their corresponding volumetric sensor group (red). **(b)**: connections between two volumetric sensor groups (yellow, red).

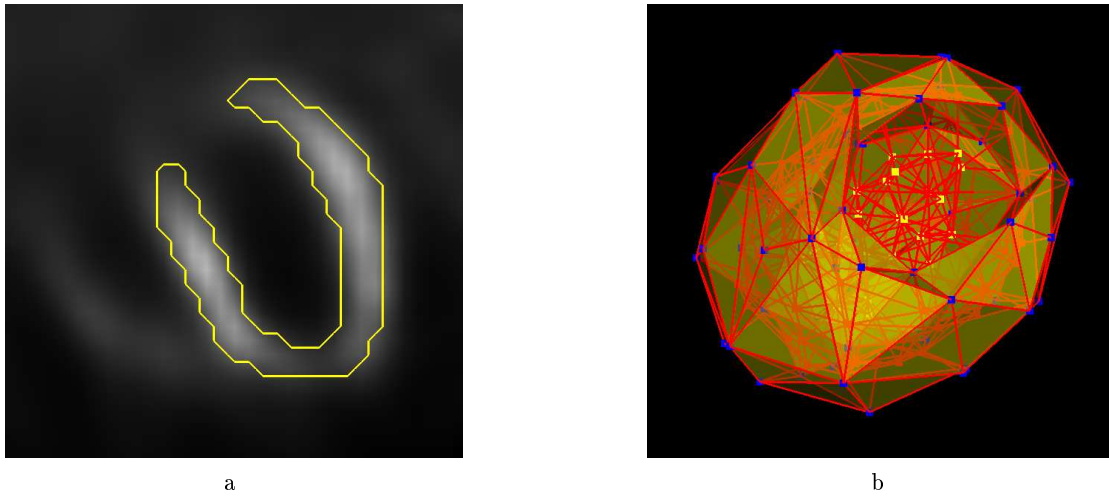


**Figure 6.** **(a)**: 2D slice of a manual segmentation bridging a functional gap in the bottom of the LV wall (darker part within the segmentation). **(b)**: generated model in 3D view.

The model should consist of two volumetric submodels for the white LV wall region and the black LV interior region (see figure 1c). Additionally, there should be a surface submodel for the LV wall border modelling.

From a manually chosen sample segmentation, which should be an average representative of all LVs in the different datasets, we generated an SMSM automatically (figure 6b) in 6 seconds on a modern PC (Pentium 4, 3.2 GHz). The generated model consisted of 153 sensors, 630 springs and 124 faces. Cross-linking was local. The average degree of cross-linking of a mass was approximately 8.7. This is a sparse crosslinking, but still too complex for manual creation for this sensor count.

We used this model successfully for automatic segmentation of the left ventricle in myocardial perfusion SPECT datasets.<sup>11</sup> The quality of the automatic segmentation lies within the range of the quality of manual comparison segmentations.

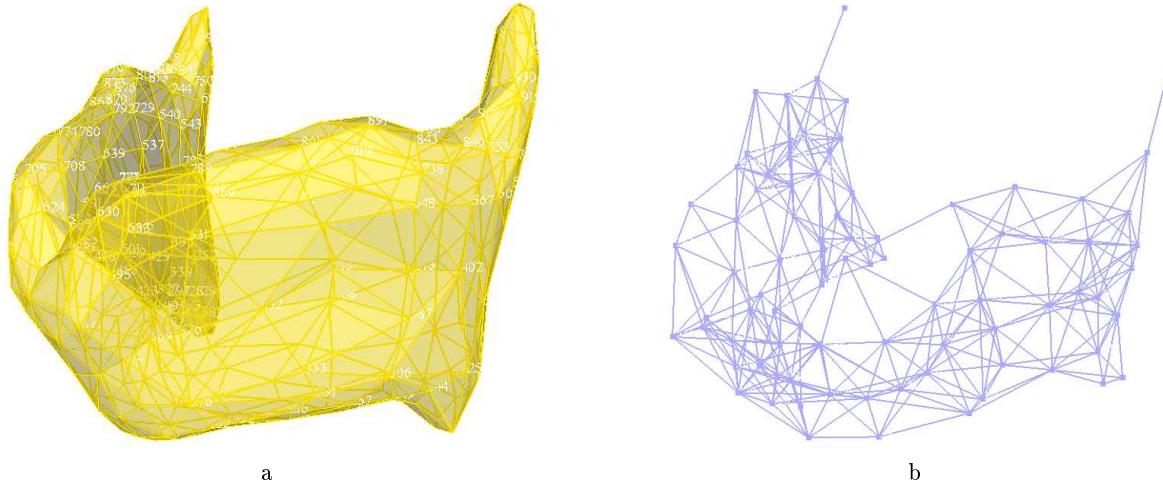


**Figure 7.** Automatically generated model for the thyroid cartilage: (a) surface submodel. (b) volumetric submodel.

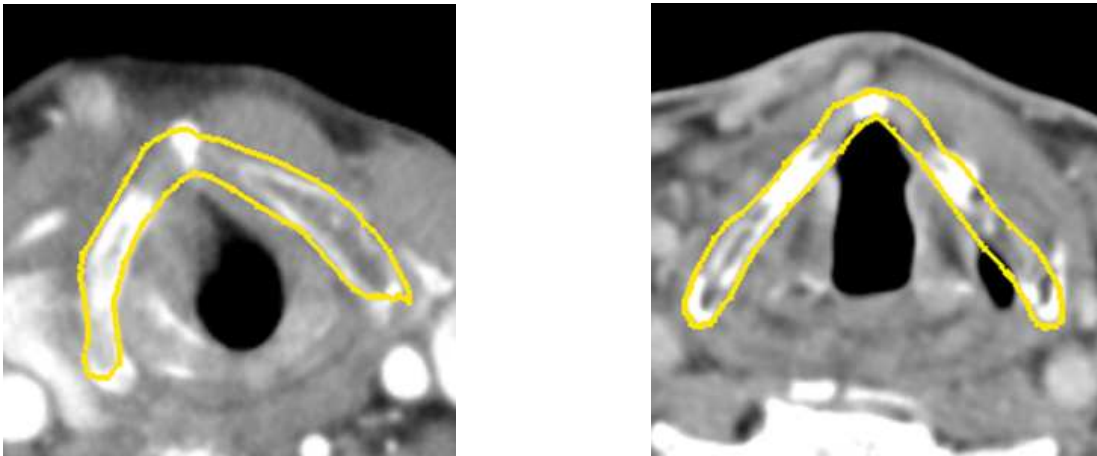


**Figure 8.** Segmentation results with the generated model of the thyroid cartilage.

## 6.2. Thyroid cartilage segmentation in CT

We applied the same methods and strategies for model generation to the application of segmenting the thyroid cartilage in CT. Here, a model-based segmentation was necessary, due to the inhomogeneous and incomplete depiction of the larynx in CT data. The shape of the cartilage is significantly more complex than that of the left ventricle and no inner region with significant appearance can be used. So only two submodels were used: the volumetric model for the thyroid cartilage region and the corresponding surface model representing its boundary.

The automatic model generation for the thyroid cartilage is based on a manual segmentation created from a dataset with a visually average-shaped larynx. The generated model represents the abstract shape of a thyroid cartilage well, preserving special features like the cornu superii and inferii (figure 7).

For our examination, 11 CT datasets of the larynx were available. For all these datasets, the segmentation using the model was successful with only minor manual user corrections. The model was placed in the dataset by elastic initialization based on six landmarks,<sup>12</sup> which allowed for a good model initialization despite the high shape variability of the structure. The segmentation process was robust; holes and inhomogeneities in the cartilage wall were successfully bridged by the model, as figure 8 shows.

## 7. CONCLUSIONS

The generated models were adequate for the segmentation of 3D medical structures in two different cases (left ventricle and thyroid cartilage) (requirements (a) - (c) from section 4). In fact, automatic model generation was essential, since such models could not be created by hand, because of the needed size, dimensionality and exactness.

The model generation relies only on one sample segmentation (including the corresponding dataset) making this model-based approach also feasible for segmentation tasks with nearly no training data. The abstraction level of the generated model is configurable by several parameters during model generation and the whole generation is automatic and fast (requirements (I) - (III) from section 4), as shown in section 6.

The sample segmentation was chosen manually in each case. It seems to be an advantage, if it has an average shape with regard to all samples. The internal force weighting parameters in the following segmentation process were also chosen manually and represent the allowed variation of the mean shape determined by the model's rest shape. So, the class of structures that can be modelled by one model can be described by a mean and different variation parameters.

Finally, the model knowledge does not rely only on contour or surface information, but also on volumetric regions, which leads to more robust and straight segmentations. Furthermore, the presented generic model generation technique is independent of the application case and the kind of data, but can be adapted to each single task's requirements.

## REFERENCES

1. T. F. Cootes, C. J. Taylor, D. H. Cooper, and J. Graham, "Active shape models - their training and application," *CVIU* **61**(1), pp. 38–59, 1995.
2. M. Kass, A. Witkin, and D. Terzopoulos, "Snakes: Active contour models," *IJCV* **1**(4), pp. 321–331, 1988.
3. L. Dornheim, K. D. Tönnies, and J. Dornheim, "Stable dynamic 3d shape models," in *ICIP*, 2005.
4. A. Nürnberger, A. Radetzky, and R. Kruse, "Using recurrent neuro-fuzzy techniques for the identification and simulation of dynamic systems," *Neurocomputing* **36**, pp. 123–147, 2001.
5. R. Pohle, *Computerunterstützte Bildanalyse zur Auswertung medizinischer Bilddaten*. Habilitationsschrift, Fakultät für Informatik, Otto-von-Guericke-Universität Magdeburg, 2004.
6. H. Delingette, "Initialization of deformable models from 3D data," in *ICCV*, pp. 311–316, 1998.
7. L. Ferrarini, H. Olofsen, M. A. van Buchem, J. H. Reiber, and F. Admiraal-Behloul, "Fully automatic shape modelling using growing cell neural networks," in *MICCAI*, 2005.
8. M. R. Kaus, V. Pekar, C. Lorenz, R. Truyen, S. Lobregt, and J. Weese, "Automated 3d pdm construction from segmented images using deformable models," *IEEE Transactions on Medical Imaging* **22**(8), pp. 1005–1013, 2003.
9. M. Garland and P. S. Heckbert, "Surface simplification using quadric error metrics," in *SIGGRAPH*, pp. 209–216, 1997.
10. L. Dornheim, J. Dornheim, H. Seim, and K. D. Tönnies, "Aktive Sensoren: Kontextbasierte Filterung von Merkmalen zur modellbasierten Segmentierung," in *Bildverarbeitung für die Medizin*, 2006.
11. L. Dornheim, K. D. Tönnies, and K. Dixon, "Automatic segmentation of the left ventricle in 3d spect data by registration with a dynamic anatomic model," in *MICCAI*, 2005.
12. J. Dornheim, L. Dornheim, B. Preim, K. D. Tönnies, I. Hertel, and G. Strauss, "Stable 3d mass-spring models for the segmentation of the thyroid cartilage," tech. rep., Otto-von-Guericke-Universität Magdeburg, Germany, 2005.